GEOFISICA INTERNACIONAL

REVISTA DE LA UNION GEOFISICA MEXICANA, AUSPICIADA POR EL INSTITUTO DE GEOFISICA DE LA UNIVERSIDAD NACIONAL AUTONOMA DE MEXICO

Vol. 19 México, D.F., 1o. de enero de 1980 Núm.1

TWO-DIMENSIONAL, TIME-DEPENDENT MHD SIMULATION OF THE DISTURBED SOLAR WIND DUE TO REPRESENTATIVE FLARE-GENERATED AND CORONAL HOLE-GENERATED DISTURBANCES[1]

M. DRYER*,
S. T. WU**,
S. M. HAN**

(Received Jun.30, 1980)

RESUMEN

Un modelo numérico bidimensional magnetohidrodinámico (MHD) es usado para simular diferentes tipos de interacciones de corrientes de plasma de alta velocidad con un flujo ambiental no perturbado de viento solar. Los orígenes físicos de estos tipos de interacción se especifican suponiendo que las corrientes de plasma de alta velocidad se generan por medio de dos fenómenos forzados: (i) una liberación de energía limitada en el tiempo y representada por un destello solar transitorio; (ii) una corriente de plasma de alta velocidad generada en un agujero coronal recién creado, la cual continúa, sin disminuir, entregando energía al flujo original del viento solar. Debido a la diferencia en la escala de tiempo del destello solar y del agujero coronal, el desarrollo del flujo perturbado detrás de los frentes de choque generados en el destello y en el agujero coronal es distinto. Esto es, el último puede iniciarse en una escala de tiempo de un día, pero puede continuarse por una o más rotaciones solares. Por otra parte, el primero puede

[1] This paper was presented at the SCOSTEP/IAU/COSPAR/IAGA Solar-Terrestrial Physics Symposium, June 1978, in Innsbruck, Austria, under the title: "Two-dimensional MHD Simulation of Stream Interactions due to Solar-Flares and Newly-Created Coronal Holes.

* *Space Environment Laboratory National Oceanic and Atmospheric Administration Boulder, Colorado 80303, USA*

** *The University of Alabama in Huntsville, Huntsville, Alabama 35807, USA*

iniciarse solamente en una escala de tiempo de minutos o hasta una hora, después del cual su decaimiento se mide en una hora o dos más. Por lo tanto, hemos iniciado un estudio de estas dos causas variando simplemente la duración temporal de los disturbios en el cálculo del valor inicial. Varias diferencias en el comportamiento dinámico de la interacción del viento solar con un frente de choque generado en un agujero coronal, y con el generado en un destello solar se hacen notar en este estudio. En el primer caso, un resultado único es el desarrollo de una burbuja magnética que viaja hacia afuera.

ABSTRACT

A two-dimensional, time-dependent, magnetohydrodynamic (MHD), numerical model is used to simulate several types of high speed stream interactions with an ambient, undisturbed solar wind flow.The physical origins of these two types of interactions are achieved by assuming that the high speed streams are generated by the occurrence of two "forcing" phenomena: (i) a temporally-limited energy release represented by a transient flare; and (ii) a newly-created, coronal hole-generated high speed stream which continues, unabated, to add energy into the original, background solar wind flow. Because of the difference in the time scales of a flare and an evolving coronal hole, the development of the disturbed flow behind flare-generated and coronal-hole-generated shocks is different. That is, the latter can be initiated on a time scale of a day but can continue for one or more solar rotations. The former can be initiated on only a time scale of minutes or an hour after which its decay is measured within another hour or two. Therefore, we have initiated a study of these two cases by simply varying the time duration of the disturbances in the initial-value calculation. Thus, several differences in dynamical behavior for the solar wind interaction with a coronal-hole-generated shock and that due to a flare-generated shock are exhibited in this study. In the former case, a unique result was the development of an outward-travelling magnetic "bubble".

1. INTRODUCTION

Recent progress in numerical simulation of shock propagation in the solar wind has been substantial. It has been improved from a simple one-dimensional hydrodynamic (HD) time-dependent, model (Hundhausen, 1973*a*, *b*) to a two-dimensional, time-dependent, magnetohydrodynamic (MHD) model (Wu *et al.*,1979). Certainly, each of these models has its specific assumptions and physical consequences which represent certain aspects of physical problems in HD and MHD problems in space plasma physics. For example, Hundhausen (1973*a*) and Dryer and Steinolfson (1976) have utilized the one-dimensional, time-dependent, HD and MHD models, respectively, to study high speed solar wind streams and large-scale solar wind evolution. Wu *et al.* (1976) studied the propagation of flare-generated shocks for the June-July 1972 solar events by using a one-dimensional time-dependent, HD model. Most recently, Wu *et al.* (1979) have used a two-dimensional time-dependent, MHD model to simulate multiple high-speed solar wind interactions. This two-dimensional model has already been applied by D'Uston *et al.* (1981) to simulate major features of a flare-generated disturbance at widely-separated positions in solar helio-longitude. The intent of this research is to study the cause-and-effect (in the solar equatorial plane) via an iterative process, when appropriate. Intriligator (1980) and Burlaga *et al.* (1980) have provided a wealth of recent examples of multi-spacecraft observations by Helios, Voyager, Pioneer, and Imp spacecraft of disturbances

in the solar wind caused by solar flares and transient coronal holes. There are many more examples. For a review, the reader is referred to Dryer (1975).

In the present paper, we continue this demonstration of representative temporal phenomena and shall present numerical results from the basic MHD numerical model of Wu *et al.* (1979). The results are initiated mathematically by using different boundary perturbation conditions which correspond to different representative physical situations. That is, in our first example, we will simulate the two-dimensional disturbance in the interplanetary (solar equatorial) medium produced by a flare-generated shock wave. In the second example, we will simulate the interplanetary disturbance produced by a newly-created coronal hole-generated high speed stream which is maintained indefinitely. We will neglect solar rotational and latitudinal effects in both examples. In Section 2, we summarize the basic physical laws for the model and describe the initial and boundary conditions. Numerical results for the flare- and coronal hole-generated disturbances are discussed in Section 3, and our concluding remarks are offered in Section 4.

2. BASIC THEORY AND NUMERICAL PROCEDURES

2.1. *Governing equations*

The assumptions made in this study are identical to those given by Wu, Han and Dryer (1979). Thus the governing equations are the same. However, for the convenience of numerical computation, we have recast the governing equations in a quasi-conservation form in spherical coordinates (r, θ, ϕ) and specialized for the equatorial plane ($\theta = 90^{\circ}$) as discussed by Han (1977). Therefore, we will not consider latitudinal effects (i.e., $\partial/\partial\theta = 0$) which *may* be present in a time-dependent three-dimensional case. Thus, the general equation for the conservation of fundamental physical quantities is given in Eq. (1):

$$\frac{\partial \mathbf{W}}{\partial t} + \frac{\partial}{\partial r}\mathbf{F} + \frac{1}{r}\frac{\partial}{\partial \phi}\mathbf{G} = \mathbf{S}, \tag{1}$$

where

$$\mathbf{W} = \begin{bmatrix} r^2\rho \\ r^2\rho V_r \\ r^2\rho V_\phi \\ rB_r \\ rB_\phi \\ r^2\left(\dfrac{1}{\gamma-1}P + \dfrac{1}{2}\rho|\mathbf{V}|^2 + \dfrac{|\mathbf{B}|^2}{2\mu_0}\right) \end{bmatrix}, \tag{2}$$

$$\mathbf{F}=\begin{bmatrix} r^2\rho V_r \\ r^2\left(p+\rho V_r^2+\dfrac{B_\phi^2-B_r^2}{2\mu_0}\right) \\ r^2\left(\rho V_r V_\phi-\dfrac{B_r B_\phi}{\mu_0}\right) \\ 0 \\ r(V_r B_\phi - V_\phi B_r) \\ r^2\left\{V_r\left(\dfrac{\gamma}{\gamma-1}p+\dfrac{1}{2}|\mathbf{V}|^2\right)-\dfrac{B_\phi}{\mu_0}(V_\phi B_r - V_r B_\phi)\right\} \end{bmatrix} \tag{3}$$

$$\mathbf{G}=\begin{bmatrix} r^2\rho V_\phi \\ r^2\left(\rho V_r V_\phi-\dfrac{B_r B_\phi}{\mu_0}\right) \\ r^2\left(p+\rho V_\phi^2+\dfrac{B_r^2-B_\phi^2}{2\mu_0}\right) \\ r(V_\phi B_r - V_r B_\phi) \\ 0 \\ r^2\left\{V_\phi\left(\dfrac{\gamma}{\gamma-1}p+\dfrac{1}{2}\rho|\mathbf{V}|^2\right)+\dfrac{B_r}{\mu_0}(V_\phi B_r - V_r B_\phi)\right\} \end{bmatrix} \tag{4}$$

and

$$\mathbf{S}=\begin{bmatrix} 0 \\ 2rp+r^2\rho\dfrac{\partial\psi}{\partial r}+\dfrac{rB_r^2}{\mu_0}+r\rho V_\phi^2 \\ \dfrac{rB_r B_\phi}{\mu_0}+r\rho\dfrac{\partial\psi}{\partial\phi} \\ 0 \\ 0 \\ r^2\rho\left\{V_r\left(\dfrac{\partial\psi}{\partial r}+\dfrac{1}{r}\dfrac{\partial\psi}{\partial\phi}\right)\right\} \end{bmatrix}, \tag{5}$$

The first term in Eqs. (2) through (5) gives the continuity equation. The second and third terms give the momentum equations in the radial and azimuthal directions, respectively. The fourth and fifth terms give the induction equation with infinite conductivity, governing the interaction between the plasma motion and the magnetic field. Finally, the sixth term provides the energy conservation equation. This dynamical system is assumed to be adiabatic and dissipationless (except at shocks). The symbols have their usual meaning: ρ denotes the mass density; $V = (V_r, 0, V_\phi)$ denotes flow velocity vector; T denotes temperature; $B = (B_r, 0, B_\phi)$ denotes the magnetic field; $p = \rho RT$ being the gas pressure; ψ the gravity potential; γ the specific heat ratio; and, finally, μ_0 the magnetic permeability in a vacuum. The independent variables are time (t) and the two-dimensional radial (r) and azimuthal (ϕ) coordinates.

2.2 Initial/Boundary Conditions

The initial boundary conditions are the same as those used in the work of Wu *et al.* (1979) in which a steady, radially-dependent solar wind, with a representative spiral magnetic field configuration, is used. The magnitude of this solar wind is found by setting $\partial/\partial t = 0$ in Eq. (1) and specifying representative parameters at 1 AU. The steady-state solution is not carried through the critical points since we are interested in this study only in the outer flows. Our steady solar wind is similar to the solution obtained by Weber and Davis (1967). Specifically, the resulting boundary conditions at the inner boundary at 18 R_S (R_S being the solar radius) are: ρ_O = 4.4 x 10^{-21}gm cm^{-3} (n_O = 2.6 x 10^3 cm^{-3}); T_O = 1.06 x 10^6K; radial velocity V_{RO} = 250 km s^{-1}; azimuthal velocity $V_{\phi O}$ = 3.3 km s^{-1}; radial magnetic field B_{RO} = 300 γ; and the azimuthal magnetic field $B_{\phi O}$ = 10 γ, where the negative sign indicates an eastern polarity in the usual Archimedian sense. The conditions at 1 AU (where 1 AU = 1 Astronomical Unit = 215 R_S) for density, temperature, and radial and azimuthal values of bulk velocity and magnetic field, respectively, are as follows: 2.2 x 10^{-23} gm cm^{-3} ($\sim$ 13 cm^{-3}), 3.1 x 10^{4}°K, 359 km s^{-1}, 0.29 km s^{-1}, 2.15 γ and -0.82 γ. From these conditions, we realize that the flow motion still is dominated by radial motion, and the magnetic field has a spiral angle of $\sim$ 21° which is a representative deviation at 1 AU from the so-called "classical" value of 45°.

2.3. *Perturbed Boundary Conditions*

The perturbed boundary conditions (i.e., $t > 0$) are chosen to be the shock jump conditions. Since the inner (i.e., low corona) boundary is outside each of the critical points, we are able to specify combined density, velocity, temperature and magnetic field disturbances according to the magnetohydrodynamic Rankine-Hugoniot shock jump conditions (Han *et al.*, 1979). The initial ordinary gasdynamic Mach and Alfvén Mach numbers are 8.68 and 8.20, respectively. The shock velocity is 1300 km/sec. These disturbances are set at the lower boundary of 18 R_S. Physically, these mathematical disturbances can be interpreted as a shock wave that is generated by either a flare or by an intensive coronal-hole-generated high-speed stream. These two cases will be distinguished by time duration of their imposition at the lower boundary. Thus, the temporal duration, τ, of the flare-generated shock disturbance is taken to be relatively short (τ = 1 hr.). On the other hand, the evolving coronal-hole-generated shock disturbance may be considered just like that for the flare except for the fact that the time duration is allowed to persist as long as the simulated time duration of the entire computation itself ($\tau = \infty$).

The properties at the outer boundary are those established by the steady-state

solar wind solution as discussed above. Our two examples are obviously idealized, but we believe that they will provide insight to spatially and temporally changing physical properties in the solar wind as a global response to two extreme cases within the class of an infinite number of possible solar disturbances.

2.4. *Numerical Procedures*

The grid points of the numerical computation are identically arranged as described in our previous work (Wu *et al.*, 1979). Because of the limitation of computer capacity, we designed our numerical system in the radial direction (as represented by the index "i") in the following way: between the lower boundary (18 R_S) and an intermediate radial position (r = 86 R_S) the grid size, Δr, was taken to be 2 R_S. Thus, a total of 35 points (i.e., $1 \leqslant i \leqslant 35$) are needed. Then, within the region from 86 R_S to 222 R_S ($\sim$ 1 AU), Δr was increased to 4 R_S. The procedure again required a total of 35 points (i.e., $i_{max} = 70$). The calculation is performed consecutively within each region; thus, results at i = 35 from the first region are stored and initialized for the next region's calculation with increasing time. This arrangement allows us to use the computer capacity effectively and resolves the problem of storage limitation. This process can be repeated, thereby allowing calculations to an unlimited radial as well as azimuthal extent. The azimuthal direction is represented by the index "j". A total of 30 radial grid arrays are utilized. Adjacent arrays are 2^o apart, thus the azimuthal distance, $r\Delta\phi$, varies from 0.63 R_S at the lower boundary ($\sim$ 18 R_S) to $\sim$ 7.7 R_S at the outer boundary of 1 AU, thus, the domain of simulated heliographic longitude is 60^o for the present computation.

The numerical computation is started with the introduction of perturbed boundary conditions as discussed in the previous sub-section (2.3). The numerical results are reported in the following section.

3. NUMERICAL RESULTS

The following discussion is divided into two parts: flare-generated disturbance (3.1) and evolving coronal-hole-generated disturbance (3.2).

3.1. *Flare-Generated Disturbance*

In this case, the numerical results are obtained for a short duration (τ = 1 hr.) shock disturbance at the lower boundary over a spatial extent of 8^o in longitude, centered within our 60^o longitudinal domain. As mentioned above, this physically corresponds to a flare-generated disturbance. Fig. 1 shows the three-dimensional representation of the normalized temperature change ($\frac{\Delta T}{T_o}$) and density change

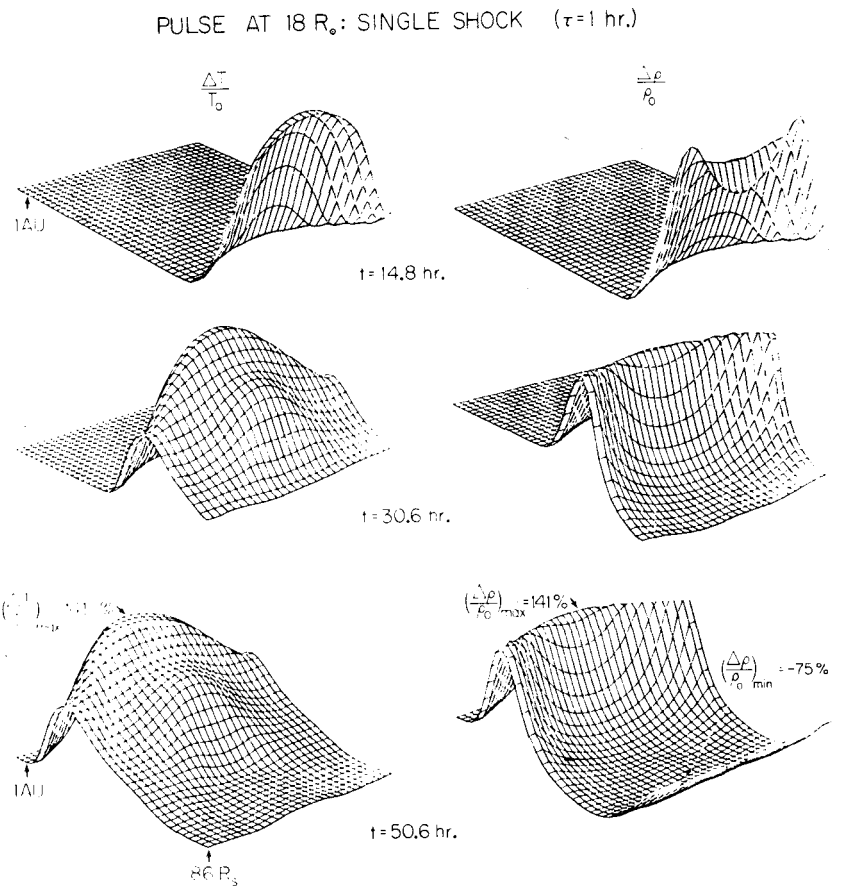

Fig. 1 Three-dimensional display (in Cartesian coordinates) of disturbed, normalized, temperature enhancement ($\Delta T/T_O$), left side, and density enhancement ($\Delta\rho/\rho_O$), right side, within the solar equatorial domain from 86 R_S to 1 AU at approximately 15 hrs., 31 hrs. and 51 hrs. after introduction of a solar flare-generated shock disturbance of duration τ = 1 hr. at the lower boundary of 18 R_S. Heliocentric radius is plotted to the left, solar longitude (60° domain) to the right, and amplitude is plotted vertically.

($\frac{\Delta\rho}{\rho_O}$) at 15 hrs., 31 hrs. and 51 hrs. after the introduction of the disturbance at 18 R_S; the disturbed region shown here extends from 86 R_S to 1 AU. The evolution and propagation of the disturbance is already clearly indicated after one day. For example, at t = 31 hrs., the two-dimensional interaction of the flare-generated shock with the initial, steady state solar wind produces, as expected, the peak rise of temperature and density. For our example, the temperature maximizes after 51 hrs. near 1 AU at ~ 1400 % of its steady-state value at that location near the

central meridian of the flare; the density peaks at ~ 140 %. The magnitudes of these maxima diminish as the shock becomes weaker in the azimuthal directions, both to the east and west. This compression and heating is followed by a rarefaction region in the density profile to a value as low as 75 % lower than the original value as shown in Fig. 1 at t = 51 hrs. The temperature profile also shows eventual cooling. This behavior is not in phase with the rarefaction because the plasma appears to be trying to maintain its thermal pressure near the central part of the disturbance. The impulsive momentum transfer to the ambient solar wind cannot, of course, be maintained, and the temperature eventually also falls below its original values before finally recovering to the ambient state. This behavior has already been demonstrated in the one-dimensional HD and MHD models (see, respectively, Wu *et al.*, 1976, and Dryer and Steinolfson, 1976). In separate computations (not shown), the longitudinal extent of the global disturbance is governed, as expected, by the longitudinal width and magnitude of the flare-generated shock introduced at the lower (18 R_S) boundary.

Fig. 2 shows the vector field of the disturbed solar wind velocity ($\Delta\vec{V} = \vec{V} - \vec{V}_O$) and magnetic field ($\Delta\vec{B} = \vec{B} - \vec{B}_O$) for t = 15 hrs., 31 hrs. and 51 hrs. in the region from 86 R_S to ~ 1 AU after introduction of the shock disturbance at 18 R_S. The decrease in magnetic field magnitude within the disturbance (i.e., behind the initial shock enhancement) is clearly shown. The magnetic polarity is always outward as indicated by several representative vectors. Note that the polarities on the eastern side of the flare central meridian undergo (at least) a single oscillation before returning to the pre-flare spiral. Furthermore, we plot in Figure 3 the normalized change of magnetic field ($\Delta\vec{B}/|\vec{B}_O|$) fifty hours after introduction of the short duration (τ = 1 hr.) flare-generated shock disturbance. This presentation shows more clearly the interaction of the asymmetrical MHD shock with the ambient medium within the domain from 86 R_S to 1 AU. It clearly indicates that an asymmetrical MHD shock has already reached 1 AU. Figure 3 also shows that regions exist within the disturbance where the magnetic field magnitude is *decreased* from its undisturbed value. The compression of the magnetic field is greater on the westernmost side of the shock because of the initial Archimedian spiral shape; that is, the jump in B_ϕ is larger on the west relative to that on the eastern side of the shock because of the initial quasi-perpendicularity of the shock on the west compared with its quasi-parallel character on the eastern side. Note, also, that the polarity changes (on both sides of the shock's central meridian) toward the center of the disturbance as noted above in the discussion of Figure 2. In the region from 18 R_S to 86 R_S, the solar wind velocity has nearly returned at t = 51 hrs. to the initial state, but the disturbance has caused a longitudinally asymmetrical change in magnetic field magnitude as the initial Archimedian spiral is temporarily, but drastically, disturbed. Although we are unable to show any latitudinal polarity disturbances, we suggest that they, too, would occur if the initial polarity of B_θ were either northward or southward (as in the case of a warped solar current sheet).

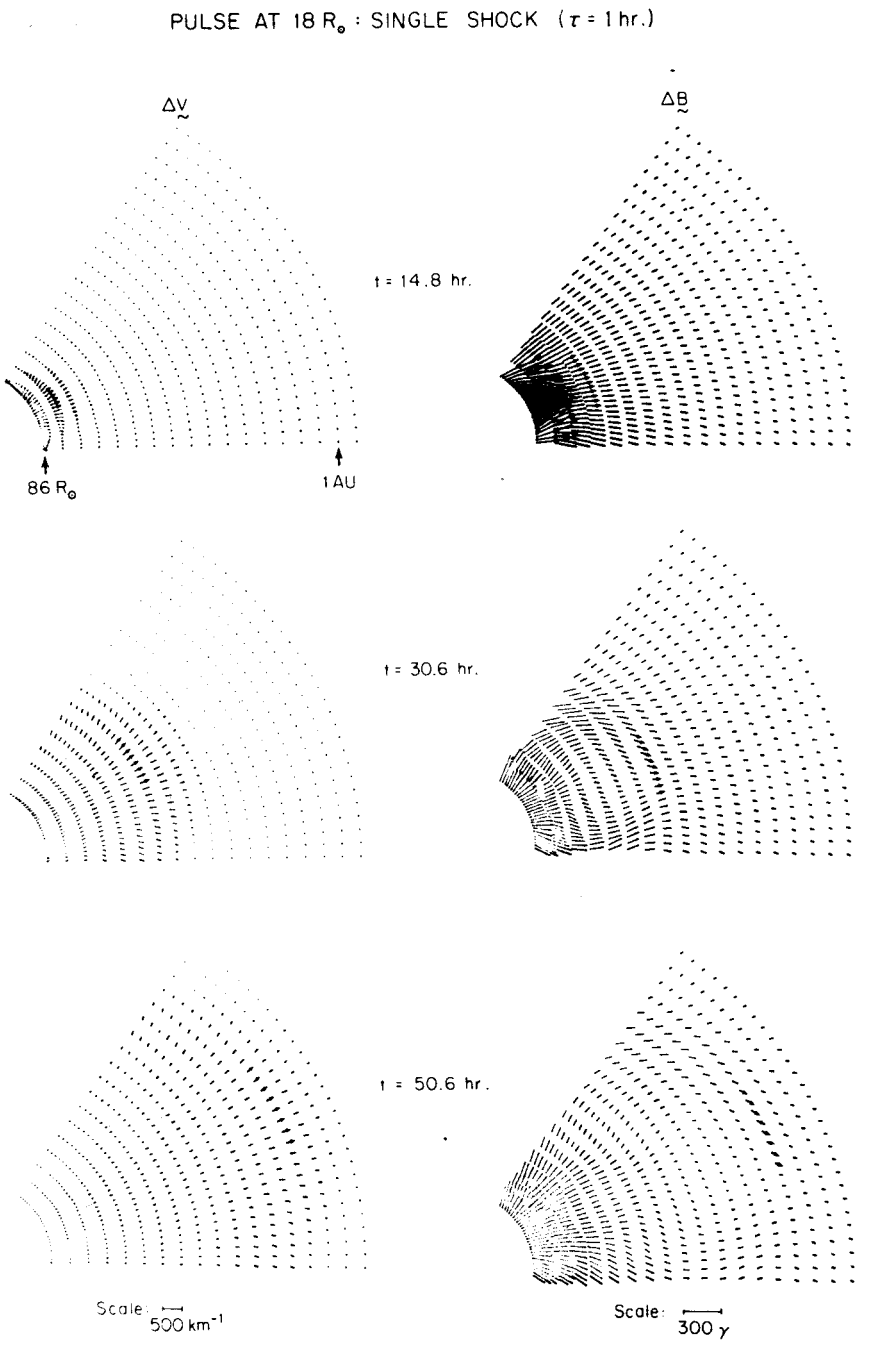

Fig. 2 - Disturbed vectorial velocity field enhancement ($\Delta V = V - V_o$) and magnetic field enhancement ($\Delta \bar{B} = B - \bar{B}_o$) for the flare-generated shock described in Figure 1 and in the text. The heliocentric radial extent (from 86 R_s to 222 R_s) and solar equatorial longitude ($\Delta\phi = 60^o$) are shown in polar coordinates. Polarities of the disturbed velocity (left) and magnetic field (right) vectors are indicated on several representative disturbed vectors. At t $\approx$ 31 hrs. note that the magnetic field polarities to the "east of the flare" reverse their polarity in accordance with shock compression requirements. This bubble-like effect is only temporary, as shown at t $\gtrsim$ 51 hrs. The scales are shown at the bottom of the figure.

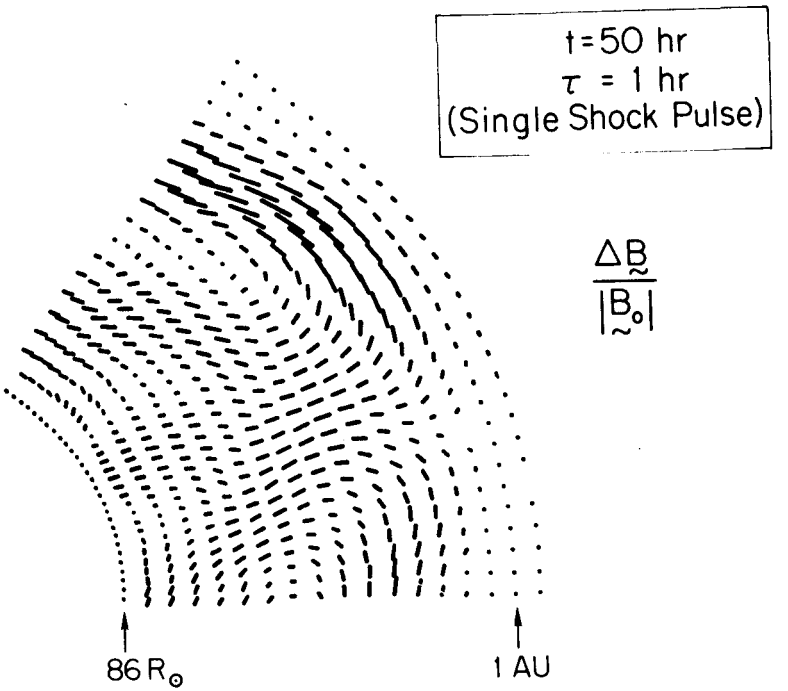

Fig. 3 Normalized vectorial magnetic field enhancement ($\Delta B/|B_o|$) in the domain from 86 R_S to 1 AU at t ≈ 50 hrs. after introduction of a flare-generated shock at 18 R_S.

3.2. *Evolving coronal-hole-generated disturbance*

We now discuss the numerical results for the long duration disturbances. That is, we "turn-on" the 1300 km/sec shock at t = 0 over the 8° longitudinal extent at 18 R_S and proceed to inject energy for an indefinite period ($\tau = \infty$). Physically, this long-lasting disturbance may represent the transient evolution of a very rapid (admittedly, extremely so) high speed stream which issues from a newly-created coronal-hole generated disturbance. The magnitude of the disturbance is probably unrealistically high since it is the same as that used for the flare-generated disturbance. The physics, however, has been appropriately incorporated in our model such that it can demonstrate (via normalized and vectorial changes of the velocity and magnetic field) the disturbance caused by continuous energy addition to the original, undisturbed solar wind. Figure 4 shows, within the 60° equatorial domain from 18 R_S to 86 R_S, the three-dimensional plots for the normalized temperature change

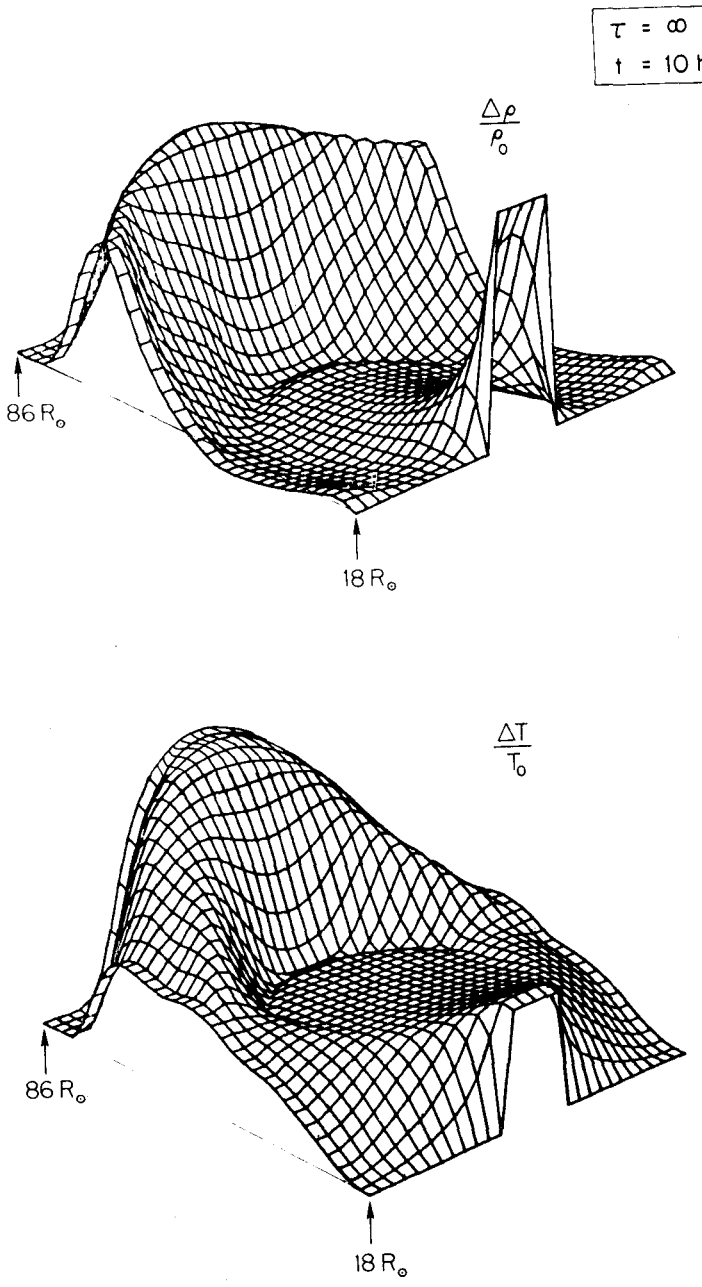

Fig. 4 Three-dimensional display (in Cartesian coordinates) of disturbed, normalized temperature enhancement, $(\Delta T/T_0)$, and density enhancement, $(\Delta\rho/\rho_0)$, within the solar equatorial plane from 18 R_S to 86 R_S at t = 10 hr. after introduction of a sustained ($\tau = \infty$) high-speed stream (preceded by a shock wave) from a newly-created coronal hole. Since no solar rotation is considered, a more realistic display would show a slight ($\sim 6^o$) skewing of the input pulse to the left because of the solar angular rotation rate of 13.5^o per 24 hr.

($\frac{\Delta T}{T_o}$) and density change ($\frac{\Delta \rho}{\rho_o}$) at 10 hrs after introduction of the disturbance. It is seen that the initial compression is again followed by a rarefaction in spite of the fact that energy and momentum continue to be injected at the inner boundary. This result clearly demonstrates the fundamental process of nonlinear MHD, large-amplitude waves (including shocks) regardless of the temporal mode of the initiating disturbance. Comparison of Figure 4 with Figure 1 clearly shows the differences between the disturbance with long duration ($\tau \rightarrow \infty$; the evolving "coronal-hole-generated" disturbance) and the disturbance with short duration (τ = 1 hr; the "flare-generated" disturbance). In the latter case (flare-generated shock), the thermal pressure attempts to compensate, with temporary success, for the diminution of the kinetic energy. In the former case (the newly-created, sustained high speed stream), the kinetic energy continues to dominate the flow and the thermal energy plummets immediately after its initial shock-induced enhancement.

A particularly interesting and completely new set of results for $\Delta\vec{V}$ and $\Delta\vec{B}$ is shown in Figure 5. This final figure shows the vectorial representation of the change of velocity and magnetic field at 10 hrs. after introduction of the disturbance. We caution again that the relative changes of magnitude and polarity, not the absolute magnitudes, are relevant for our discussion. Moreover, solar rotation (not considered) would introduce (at t = 10 hr.) only a 6^o relative skewing. The most distinctive difference between this result (apart from the obvious outward jetting and entrainment effect seen in $\Delta\vec{V}$) and that for the "flare-generated" disturbance (see Figure 2 at t $\approx$ 15 hr.) is the fact that the disturbed magnetic field in Figure 5 displays a change of polarity in the central portions of the disturbance. This behavior may be explained as follows. Since energy is continuously fed into the system, the asymmetric shock forces the polarity (as before, for the τ = 1 hr. case) to be directed toward the center as seen near 86 R_S. However, the magnitude decrease is accompanied by polarity reversal which is produced by a new current system. A magnetic void (or "bubble") region, formed together with a null point, moves outward as sustained energy and momentum continue to be added to the flow. We could not specify whether reconnection occurs since the electrical conductivity in this computation is taken to be infinite. The vectorial velocity representation shows a fountain-like behavior (as noted above) with a relatively large velocity in the center of the disturbance (like water ejected from a garden hose). This result is consistent with the three-dimensional graphical representation (Figure 4) for the density profile, which shows a flat rarefaction region in the center of the disturbance. Thus continuity of mass flux and, as discussed above, conservation of energy flux (with domination of the kinetic over the thermal energy flux) are conserved, as required. Hypothetical observations at a single point would detect a time series of data for a compression followed by a rarefaction, albeit with a fairly constant velocity, together with a complete 360^o rotation of the magnetic polarity. This kind of observation (possibly observed by Burlaga and Klein, 1980) could properly be described

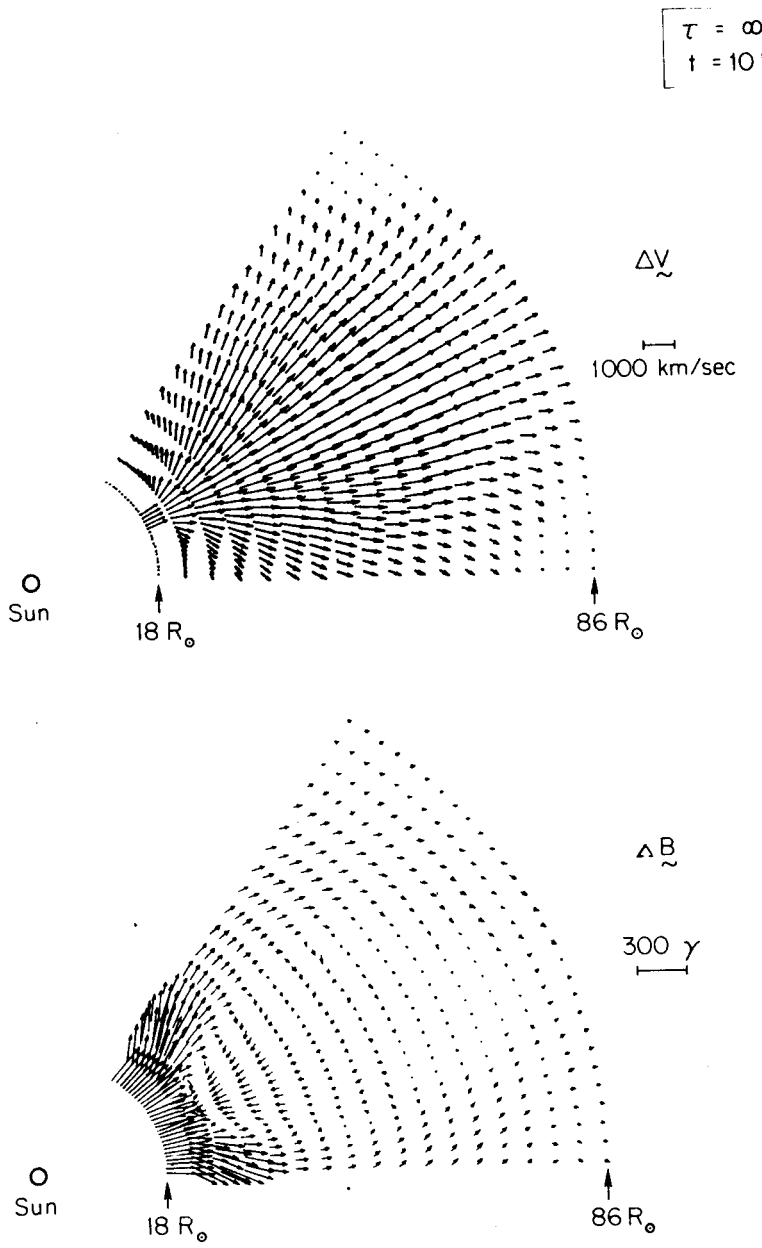

Fig. 5 Disturbed vectorial velocity enhancement ($\Delta V = V - V_o$) and magnetic field enhancement ($\Delta B = B - B_o$) for newly created coronal hole-generated shock wave described in Figure 4 and in the text. The heliocentric radial extent (from 18 R_S to 86 R_S) and solar equatorial longitude ($\Delta\varphi = 60^o$) are shown in polar coordinates at t = 10 hrs. Sustained energy and momentum input at 18 R_S is indicated by the notation, $\tau = \infty$.

as a transient "bubble" or "cloud". This topic has also been discussed by Bobrov (1979), Pudovkin *et al.* (1979), and Gosling *et al.* (1973).

4. CONCLUDING REMARKS

We have used our earlier-developed two-dimensional, time-dependent, MHD computer code (Wu *et al.*, 1979) to simulate the temporal and spatial dynamical behavior of several extreme cases of solar events. Several simple cases: (i) a short-lived solar flare and (ii) a long-lived evolution of a high-speed stream emitted from a newly created coronal hole, have been examined. Our numerical results, confined to a 60^{o} segment of the solar equatorial plane, have demonstrated a number of fundamental physical phenomena. For example, the structure of asymmetrical MHD shocks and their weakening in the azimuthal direction has clearly been shown for both cases. Also, large azimuthal velocity and magnetic field gradients, including "bubble" formation, are also shown. We believe that a theoretical description of the kind found here (and which has been speculated upon by various observers) has not been found previously. To reveal more physics of these types of dynamical behavior, the numerical model should be improved by including finite electrical conductivity; thus, the reconnection of field lines can be shown more precisely. In order to show three-dimensional "bubble" propagation, a quasi-three-dimensional (i.e., non-plane approximation) numerical code should be developed.

5. ACKNOWLEDGMENTS

Two of the authors (STW and SMH) would like to acknowledge the financial support of a National Science Foundation Grant (ATM-77-22484) and a NASA/MSFC Contract (NAS8-28097).

BIBLIOGRAPHY

BOBROV, M. S., 1979. Magnetic classification of solar wind streams, *Planet Space Sci., 27,* 1461.

BURLAGA, L. F. and L. KLEIN, 1980. Magnetic clouds in the solar wind, (preprint), submitted to *Geophys. Res. Lett.*

BURLAGA, L., R. LEPPING, R. WEBER, T. ARMSTRONG, C. GOODRICH, J. SULLIVAN, D. GURNETT, P. KELLOGG, E. KEPPLER, F. MARIANI, F. NEUBAWER, H. ROSENBAUER, and R. SCHWENN, 1980. Interplanetary particles and fields, November 22 to December 6, 1977: Helios, Voyager, and Imp Observations between 0.6 and 1.6 AU, *J. Geophys. Res., 85,* 2227.

DRYER, M., 1975. Interplanetary shock waves: Recent developments, *Space Sci. Rev., 17,* 277.

DRYER, M. and R. S. STEINOLFSON, 1976. MHD solution of interplanetary disturbances generated by simulated velocity perturbation, *J. Geophys. Res., 81,* 5413.

D'USTON, C., M. DRYER, S. M. HAN, and S. T. WU, 1981. Spatial Structures of Flare-Associated Perturbations in the Solar Wind Simulated by a Two-dimensional Numerical MHD Model, *J. Geophys. Res.,* in press.

GOSLING, J. T., V. PIZZO, and S. J. BAME, 1973. Anomalously low proton temperatures in the solar wind following interplanetary shock waves: Evidence for magnetic bottles?, *J. Geophys. Res., 78,* 2001.

HAN, S. M., 1977. A numerical study of two-dimensional, time-dependent MHD flow, Ph. D. Thesis, University of Alabama (Huntsville).

HAN, S. M., S. T. WU, and Y. NAKAGAWA, 1979. Numerical study of an explosion in a non-homogeneous medium with and without magnetic fields, *Int'l. J. Comp. and Fluids, 1,* 97.

HUNDHAUSEN, A. J., 1973*a*. Non-linear model of high-speed solar wind streams, *J. Geophys. Res., 78,* 1528.

HUNDHAUSEN, A. J., 1973*b*. Evolution of large-scale solar wind structure beyond 1 AU, *J. Geophys. Res., 78,* 2035.

INTRILIGATOR, D. S., 1980. Transient phenomena originating at the sun – an interplanetary view, in *Solar and Interplanetary Dynamics,* Proc. IAU Symp. No. 91, (Eds: M. Dryer and E. Tandberg-Hanssen) D. Reidel Publ. Co., Dordrecht, pp. 357-374.

PUDOVKIN, M. I., S. A. ZAITSEVA, and E. E. BENEVOLENSKA, 1979. The structure and parameters of flare streams, *J. Geophys. Res., 84,* 6649.

WEBER, E. J. and L. DAVIS. Jr., 1967. The angular momentum of the solar wind, *Ap. J., 148,* 217.

WU, S. T., M. DRYER and S. M. HAN, 1976. Interplanetary disturbances in the solar wind produced by density, temperature, or velocity pulses at 0.08 AU, *Solar Phys., 49,* 187.

WU, S. T., S. M. HAN, and M. DRYER, 1979. Two-dimensional, time-dependent MHD description of interplanetary disturbances: Simulation of high speed solar wind interactions, *Planet. Space Sci., 27,* 225.